Cooperative behavior in the periodically modulated Wiener process: Noise-induced complexity in a model neutron

A. R. Bulsara
Naval Command, Control and Ocean Surveillance Center: Research, Development, Testing and Evaluation Division, Code 573, San Diego, California 92152-5000

S. B. Lowen
Department of Electrical Engineering, Columbia University, New York, New York 10027

C. D. Rees
Naval Command, Control and Ocean Surveillance Center: Research, Development, Testing and Evaluation Division, Code 541, San Diego, California 92152-5000

(Received 17 February 1994)

We consider a periodically modulated random walk (Wiener process) to an absorbing barrier with a deterministic reset to the starting point following each barrier crossing. Cooperative effects arising from the interplay between the noise and periodic modulation are analyzed as they manifest themselves in two statistical measures of the response: the passage time statistics of the process and the power spectral density of the output. Simple relationships exist between the extrema that occur in these two characterizations. The spectral properties of the response are seen to bear a striking resemblance to the *stochastic resonance* phenomenon that is known to occur in periodically driven noisy nonlinear systems.

PACS number(s): 05.40.+j

I. INTRODUCTION

The response of nonlinear dynamic systems to weak, deterministic, time-dependent stimuli in the presence of system noise has recently been of considerable interest to the statistical physics community. One of the most intriguing cooperative effects that arise out of the coupling between deterministic and random dynamics in a nonlinear system (usually taken to be bistable) is "stochastic resonance" (SR). This effect, originally reported by Benzi, Eckmann, and their co-workers [1] was proposed as a possible explanation for the Ice Ages [2]. It consists of a noise-induced enhancement of the response of a nonlinear system to a weak, external, time-periodic modulation in the presence of background noise. The signal strength, measured in the output power spectral density at the stimulus frequency, can actually be enhanced over its input value through a coherent transfer of energy between the noise and stimulus-dominated hopping dynamics between the stable attractors of the system. The mechanism of SR is simple. Given a bistable dynamic system, for example, information is transmitted through the system in the form of switching events between the stable states, or attractors, of the potential function underlying the dynamics. The effect of an applied time-periodic signal is then to rock the potential, alternately raising and lowering the wells. However, should its amplitude be very low (compared to the height of the potential barrier), it will not be able to induce switching. In the presence of even small amounts of noise (assumed throughout this work to be Gaussian and δ-correlated) there will, however, always be a finite switching probability. Since the switching probability is greater when the system is in the "elevated" well, which occurs when the signal is at its maximum, one realizes that the noise-induced switching events may acquire some degree of coherence with the deterministic signal as long as certain important system parameters, notably the potential barrier height and the locations of the fixed points, are appropriately adjusted. With increasing noise, the component $S(\omega)$ of the output power spectral density at the stimulus frequency ω increases until, for a critical noise strength, the intrawell motion gives way to interwell (or hopping) motion as the major contributor to the dynamics. After this point $S(\omega)$ decreases with noise; for very large noise strengths, the switching becomes noise dominated and very rapid, with all coherence with the periodic signal being destroyed. For modulation frequencies comparable to the Kramers rate (the characteristic well-to-well switching rate in the noise-only case), the critical noise strength (at the maximum of the signal-power curve) corresponds to a matching between the modulation frequency and twice the Kramer rate, hence the somewhat misleading characterization of this effect as a "resonance" in the physics literature. The earliest theories of SR [3] embodied adiabatic assumptions wherein the modulation frequency was taken to be smaller than the Kramers rate of the system in the absence of the modulation. Latter theories relied on systematic expansions of the response autocorrelation function in matrix continued fraction series [4] or linear response approaches [5]. The physics literature is also replete with demonstrations of SR in numerous experiments [6] and analog simulations [7]. A good overview of the phenomenon may be found in recent review articles by Moss [8] and Jung [9] as well as the proceedings of a NATO workshop on the subject [10]. Recent contributions to the field tend to focus on the role of multiplicative noise, i.e., fluctuations in the potential barrier height and locations of the minima [11], the extension of conventional theories of SR to new regimes of parameter space [12], and the interplay of noise and modulation in populations of globally coupled bistable elements [13,14].

In addition, there has been much recent speculation about the possible central role played by SR in the response of sensory neurons (modeled as bistable noise-controlled switching elements) in the mammalian nervous system [14,15].

The above paragraph provides a short survey of research carried out to date in this field, for the most part on bistable dynamic systems, i.e., systems whose dynamics can be underpinned by a double-welled "potential function." However, SR is by definition a threshold process. One assumes that the deterministic periodic modulation is too weak to cause transitions over the potential barrier in the absence of the noise; then even small amounts of added white noise will lead to noise-assisted barrier crossings, thereby enhancing the output signal-to-noise-ratio of the system. This, in turn, raises the question of whether similar cooperative effects can be seen in the response of a simpler system, quantified solely in terms of threshold crossing events. The fact that SR may indeed be a feature of signal processing by sensory neurons and that there exist simpler mathematical models of neural firing than the bistable models referred to above provides further momentum to this question. A very recent paper by Wiesenfeld *et al.* [16] describes SR in the response of a simple system, one in which a state point makes an excursion to a barrier, under the influence of white noise and a weak periodic signal; after surmounting the barrier (which is impossible without the noise) the state point is returned deterministically to its starting point. This system can be used as a prototype of a variety of "excitable systems," some of which are known to provide very good descriptions of certain properties of excitable cells. Indeed, Wiesenfeld *et al.* are able to match the predictions of their generic theory quite well with analog simulations of a Fitzhugh-Nagummo model of the neuron, as well as experimental data from the mechano receptor of the Missouri crayfish stimulated by external noise and a weak periodic modulation. The predictions match the simulations even though, unlike other single-state treatments of SR [17], they do not explicitly consider a system dynamics described by a monostable potential.

Motivated by recent work in the modeling of the response of sensory neurons to deterministic periodic signals embedded in a noise background [14,15], we wish to consider the response of simpler (compared to the plethora of bistable-system-based treatments to date) systems to such external stimuli. It seems fitting to consider continuous state space random walk models, since these embody some of the most fundamental concepts of statistical physics and can be used in modeling a wide variety of phenomena in areas as diverse as genetics and astronomy. In fact, the response of the simplest one-dimensional random walk to a time-periodic stimulus has already been described by Fletcher, Havlin, and Weiss [18]; they show that the mean residence time is a minimum for certain characteristic frequencies. Excellent reviews of random walk dynamics exist [19], and rigorous theories of the first passage time in stationary one-dimensional random walks have been developed by Siegert and his co-workers [20] (see [21] for good reviews).

The model that we consider in this work is a special case of the periodically driven Ornstein-Uhlenbeck process [22]:

$$\dot{x}=\lambda(u_r-x)+\mu+F(t)+q\cos\omega t \ . \tag{1}$$

Equation (1), in the absence of the periodic stimulus, has been extensively studied in the theoretical neuroscience literature as a so-called "integrate-fire" (IF) model of neurons [23]. In these studies, $x(t)$ represents the cell membrane voltage, with μ being a positive drift to a firing threshold a while λ is a decay constant governing the decay of the voltage variable to a resting level u_r. The noise term $F(t)$ represents the net contribution from all the synaptic inputs to the cell; it is usually taken to be Gaussian and δ-correlated with zero mean and variance D. Deterministic IF models have been studied by Keener, Hoppenstaedt, and Rinzel [24]. Excellent reviews of the applications of models such as (1) to neurophysiological modeling can be found in the works of Tuckwell [25].

In this work, we shall consider a simplification of the above model, the $\lambda=0$ case; of course, the $\lambda=0=q=\mu$ case constitutes the celebrated free-particle problem studied by Einstein [22]. Before studying the effects of the periodic stimulus, however, it is instructive to review some of the results for the unmodulated ($q=0$) case, the so-called Wiener process [21,22]. Such a model was introduced by Gerstein and Mandelbrot (GM) [26] as a model of neural firing events subject to certain constraints. In their model, which they called the "perfect integrator," the underlying dynamics are assumed to be describable by a stationary random walk based on the cornerstone requirement of a stable distribution function, in the absence of drift, for the probability density of first passage times corresponding to the dynamics. The state variable $x(t)$, representing the membrane voltage, is assumed to execute a biased random walk to an absorbing threshold a at which point a firing event is designated to have occurred, and $x(t)$ is instantaneously reset to its starting value, the reset mechanism being purely deterministic. It is this reset which renders the "global" dynamics nonlinear. It is also assumed that the motion occurs under the bias of a positive drift coefficient μ which was defined by GM as the suitably weighted difference between excitatory and inhibitory synaptic inputs (it is neurophysiologically reasonable to assume these inputs to be different [26]). For this model, the Wiener process with drift, one readily writes down the associated Fokker-Planck equation (FPE) [21,22],

$$\frac{\partial}{\partial t}P(x,t)=-\mu\frac{\partial P}{\partial x}+\frac{D}{2}\frac{\partial^2 P}{\partial x^2} \ . \tag{2}$$

From (2) the first passage times density function (FPTDF), also known in the neurophysiological literature as the interspike interval histogram (ISIH), is readily found to be [21]

$$g_0(t)=\frac{a}{\sqrt{2\pi Dt^3}}\exp\left\{-\frac{(a-a_0-\mu t)^2}{2Dt}\right\} , \tag{3}$$

a_0 being the starting point of the random walk. The density function $g_0(t)$, often referred to in the statistical

literature [27] as the inverse Gaussian, reproduces many of the properties of experimentally observed FPTDF's (for spontaneous firings) reasonably well, including the long (exponential) tail in the FPTDF $g_0(t)$. However, the model also has numerous limitations (which have been enumerated by GM), the most fundamental one being the assumption that the membrane potential is deterministically reset following each firing event; nevertheless, it provides a simple vehicle to explain, on a grossly simplified level, the dynamics that arise from the coupling of the noise to the drift-driven dynamics in certain classes of neurons. A more rigorous (from a neurophysiological standpoint) grounding of the FPE (2) has been given by Stevens [28].

The first passage time statistics corresponding to the $q=0$ case are readily calculated from the FPTDF (3). In particular, the mean first passage time (MFPT) $\bar{t} \equiv t_0 = (a-a_0)/\mu$ to the absorbing threshold is calculated as the first moment of $g_0(t)$, and its reciprocal yields an average firing rate. The variance of the first passage time is $t^2 - \bar{t}^2 = D(a-a_0)/\mu^3$. For a long-tailed distribution of the form (3), however, possibly the more important quantity is the most probable time or mode, corresponding to the maximum of the FPTDF. For the $q=0$ case, this time is readily obtained by differentiation:

$$t_m = \frac{3D}{2\mu^2}\left\{\left[1+\frac{4a^2\mu^2}{9D^2}\right]^{1/2}-1\right\}. \tag{4}$$

It is significant that the mode t_m depends on the noise. In experiments, crossing or firing times clustered about the mode are more probable. The mean of a large number of firing times may yield a MFPT t_0 which, depending on the physical characteristics of the density function (3), is close to the mode or farther out in the tail. When analyzing the properties of the FPTDF, the interplay of the three time scales $T_0 (=2\pi/\omega)$, t_0, and t_m is crucial. With increasing drift μ (corresponding in a neurophysiological context to decreasing inhibition) or with decreasing noise strength, while keeping the drift fixed, the FPTDF approaches a more sharply peaked density; in effect, the tail of the density (3) shrinks, with the mean approaching the mode. This may be demonstrated via a Gram-Charlier expansion of the density function (3), and is depicted in Fig. 1 in which we plot the ratio t_m/t_0 vs the drift μ and the noise variance D. Increasing the drift is seen to lead to a more sharply peaked distribution as $t_m/t_0 \to 1$ for a given noise variance; the approach to a very sharply peaked distribution is more rapid at lower noise strengths. In the $\mu \to 0$ limit, the mean t_0 increases without bound, corresponding to the long tail that emerges, in this limit, in the distribution function $g_0(t)$; the mode, however, approaches a limiting value $t_m = a^2/3D$. For this case, the moments of the FPTDF must be computed by invoking a cutoff t_c, i.e., we redefine the FPTDF to be the probability density of reaching the barrier in some finite time t_c; this case is not considered in this work.

In the following two sections, we detail the effects of including the periodic modulation term in the dynamics.

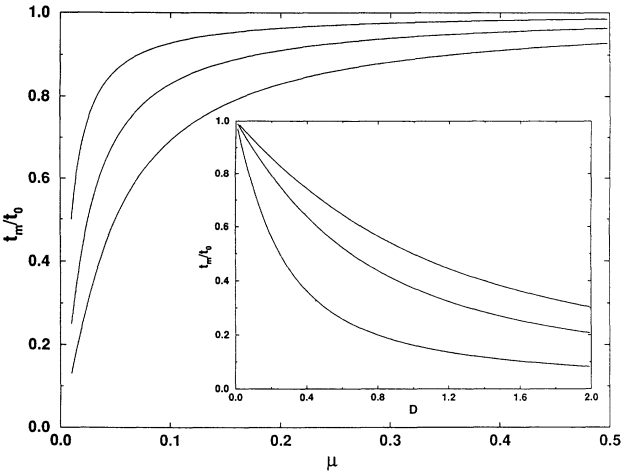

FIG. 1. Mode-to-mean ratio of the FPTDF (3) vs drift μ with noise variance (reading curves from top to bottom) $D=0.1$, 0.25, 0.5 and (inset) vs noise variance D for (reading curves from top to bottom) $\mu=0.1$, 0.0625, and 0.025. $a=20$ and $q=0$ for all curves.

The resulting FPTDF's are seen to be strikingly similar to and display many of the properties of escape time distributions that have been studied in nonlinear systems with dynamics underpinned by a bistable potential. In fact, some of the noise-induced cooperative behavior that we will observe in the FPTDF and the power spectral density of the output $x(t)$ is seen to be strikingly similar to behavior in bistable systems that has been linked to the stochastic resonance phenomenon. A detailed discussion of these points is contained in the following sections.

II. WEAK PERIODIC STIMULUS AND THE FPTDF

We now consider the inclusion of the periodic modulation term in the dynamics: the $q>0$ case of Eq. (1), but with $\lambda=0$. We require that, following each crossing of the absorbing barrier at $x=a$, a particle described by the state variable $x(t)$ is reset to its starting point $a_0=0$. We also assume that the phase difference between the solution $x(t)$ and the periodic stimulus is reset to zero following each barrier crossing. This is an important point; if we allowed the phase to remain coherent across the reset times, there would be, after an initial transient, a preferred phase at which most of the threshold crossings occurred. Thus the only effective difference between the coherent model and the full reset model would be a phase offset in the response statistics, merely a quantitative change. The FPE for our model is easily written down:

$$\frac{\partial}{\partial t}P(x,t) = -(\mu + q\cos\omega t)\frac{\partial P}{\partial x} + \frac{D}{2}\frac{\partial^2 P}{\partial x^2}. \tag{5}$$

The substitution $y = x - \mu t - (q/\omega)\sin\omega t$ enables us to solve the FPE, using the method of images, subject to the condition of the absorbing boundary at $x=a$,

$$\sqrt{2\pi Dt}\,P(x,t)=\exp\left[-\frac{[x-\mu t-(q/\omega)\sin\omega t]^2}{2Dt}\right]-\exp\left[\frac{2a}{Dt}\left[\mu t+\frac{q}{\omega}\sin\omega t\right]\right]$$
$$\times\exp\left[-\frac{(x-2a-\mu t-(q/\omega)\sin\omega t)^2}{2Dt}\right], \quad (6)$$

whence the FPTDF is computed via the prescription [21]

$$g(t)=-\frac{d}{dt}\int_{-\infty}^{a}P(x,t)dx\ ,$$

which yields, after some calculation,

$$g(t)=\frac{1}{\sqrt{2\pi D}}\frac{a}{t^{3/2}}\exp(-f_1)+\frac{aq}{Dt^2}\left[t\cos\omega t-\frac{1}{\omega}\sin\omega t\right]$$
$$\times\Phi_c(f_3)\exp(f_2)\ , \quad (7)$$

where $\Phi_c(z)\equiv(2/\sqrt{\pi})\int_z^\infty e^{-t^2}dt$ is the complementary error function and we have defined

$$f_1\equiv\frac{[a-\mu t-(q/\omega)\sin\omega t]^2}{2Dt}\ ,$$
$$f_2\equiv\frac{2a}{Dt}\left[\mu t+\frac{q}{\omega}\sin\omega t\right]\ ,$$
$$f_3\equiv\frac{[a+\mu t+(q/\omega)\sin\omega t]}{\sqrt{2Dt}}\ .$$

For future use, it is convenient to expand (7) to first order in q:

$$g(t)\approx g_0(t)+\frac{aq}{Dt^2}(t\cos\omega t-\omega^{-1}\sin\omega t)$$
$$\times\Phi_c\left[\frac{a+\mu t}{\sqrt{2Dt}}\right]\exp(2a\mu/D)\ . \quad (8)$$

For the small values of q considered in this work, this expression yields a FPTDF that is virtually identical to the exact expression (7).

We now briefly discuss some of the properties of the density function (7). The mean first passage time for the $q>0$ case could be found directly from (7) by integration. It is, however, far simpler to note that the MFPT is simply the passage time to the boundary in the absence of noise. Then, since we assume the periodic motion to be simply a small perturbation to the drift dynamics, a first-order perturbation solution of the dynamic equation $a=\mu t+(q/\omega)\sin\omega t$ yields the deterministic passage time corresponding to the MFPT for the $\lambda=0$ case of the process (1):

$$\bar{T}=t_0\left\{1-\frac{(q/a\omega)\sin\omega t_0}{1+(q/\mu)\cos\omega t_0}\right\}\ , \quad (9)$$

where $t_0\equiv a/\mu$ is the mean first passage time in the presence of noise alone. Note that $\bar{T}\to t_0$ at high drive frequencies ω, as expected. Also, in the absence of the drift, one obtains a MFPT $\bar{T}=\omega^{-1}\sin^{-1}(a\omega/q)$ which is defined only for $q>a\omega$; we do not consider this range of parameters in this work.

We now consider the temporal behavior of the FPTDF (7). At very low stimulus frequencies ($\omega\ll 2\pi/t_0$), with all the other parameters fixed, the FPTDF consists of a single narrow peak located near $t=t_m$. The motion for this case is dominated by the noise and the drift with the mean of the FPTDF being given by $\bar{T}\approx t_0(1+q/\mu)^{-1}$ which approaches t_0 for small q/μ. Increasing the stimulus frequency leads to the development of additional peaks in the FPTDF. As $\omega\to 2\pi/t_0$, the dominant peak approaches the location $t=T_0$ with smaller peaks beginning to appear near $t=nT_0$ ($n>1$). Finally, for $\omega=2\pi/t_0$, the FPTDF consists of a dominant peak located at $t=T_0$ ($=t_0$) with smaller peaks located at $t=nT_0$ ($n>1$). For stimulus frequencies greater than $2\pi/t_0$, the FPTDF exhibits peaks at locations nT_0 where n is a positive integer. Figure 2 shows the FPTDF for two choices of the drift μ; increasing the drift μ is seen to lead to a narrower FPTDF, as described in the preceding section. The FPTDF (3) corresponding to the $q=0$ case is seen to be the envelope of the more general FPTDF (7); in fact it is evident that if we adjust the stimulus and/or system parameters such that

$$t_m=nT_0\ , \quad (10)$$

then the nth peak will be the highest one. This is shown in Fig. 2 (solid curves); here, the drift μ has been adjusted to make the peak at $n=4$ the highest one.

A. Peak heights in the FPTDF

An interesting feature about the FPTDF (7) is that the peak heights go through maxima as functions of the noise variance D. This is demonstrated in Fig. 3 for a particular set of system and modulation parameters. One can calculate from (7) the critical noise D_c at which the nth peak passes through its maximum. Noting that the peaks

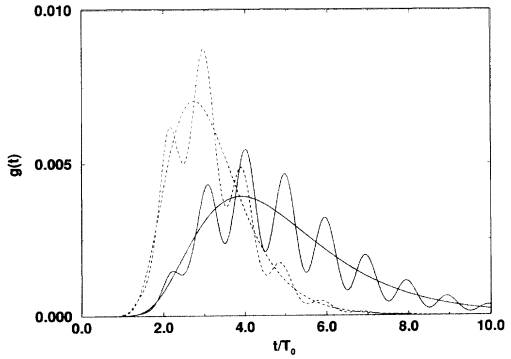

FIG. 2. FPTDF (7) vs normalized time t/T_0 for $q=0$ cases (smooth curves) and $q=0.03$, with drift $\mu=0.065$ (solid curves) and 0.1 (dashed curves). $a=20$, $\omega=0.1$, and $D=0.2$ for all curves.

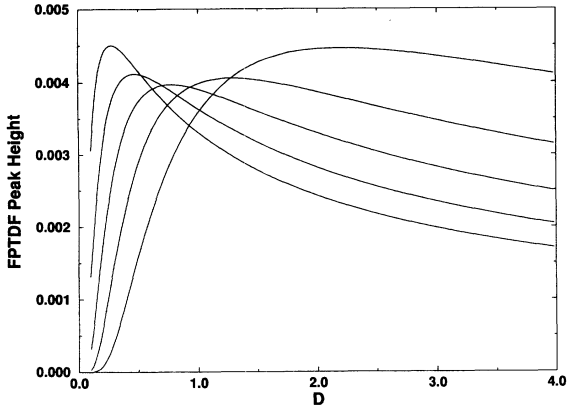

FIG. 3. FPTDF peak heights vs noise variance D corresponding to the density function (7) for peak numbers $n=7,6,5,4,3$ reading from left to right. $a=20$, $q=0.047\,53$, $\mu=0.055$, and $\omega=0.2$ for all curves.

in (7) occur at times $t=nT_0$, the amplitude of the nth peak is given by

$$h_n=h_0+h_1 \ , \tag{11}$$

where

$$h_0=\frac{a}{\sqrt{2\pi Dt_n^3}}\exp[-(a-\mu t_n)^2/2Dt_n] \ , \tag{12a}$$

$$h_1=\frac{aq}{Dt_n}e^{2a\mu/D}\Phi_c\left[\frac{a+\mu t_n}{\sqrt{2Dt_n}}\right] \tag{12b}$$

are the contributions from the $q=0$ and $q>0$ parts of the density function (7) (we set $t_n=nT_0=2n\pi/\omega$). Writing $D_c=D_{c0}+\delta$ where D_{c0} is the noise variance at which the expression (12a) is maximized and δ is the (much smaller) contribution from (12b), we easily find

$$D_{c0}=(a-\mu t_n)^2/t_n \ . \tag{13}$$

The remaining contribution δ is found by setting the derivative of (11) equal to zero and then expanding to $O(\delta)$. A somewhat tedious calculation yields

$$\delta=-\frac{A_2}{A_1+A_3} \ , \tag{14}$$

where we have set

$$A_1\equiv-\frac{a}{2\sqrt{2\pi e t_n^3 D_{c0}^5}} \ ,$$

$$A_2\equiv-\frac{aq}{t_n}e^{2a\mu/D_{c0}}(a_1b_1-D_{c0}^{-5/2}z_1e^{-p}) \ ,$$

$$A_3\equiv\frac{aq}{t_n}e^{2a\mu/D_{c0}}\left\{\frac{2a\mu a_1b_1}{D_{c0}}+a_1b_2+e^{-p}\left[z_1\left[D_{c0}^{-7/2}p+\frac{5}{2}D_{c0}^{-7/2}\right]-a_2b_1-2a\mu D_{c0}^{-7/2}z_1\right]\right\} ,$$

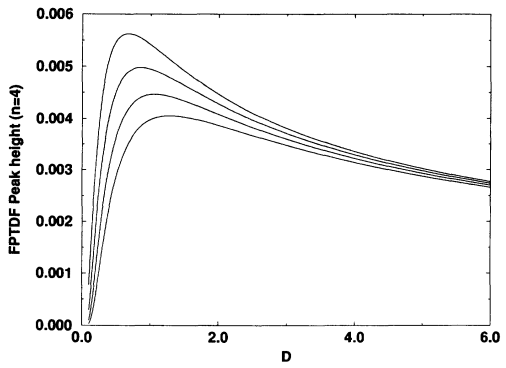

FIG. 4. FPTDF peak height of the $n=4$ peak vs noise variance D for drift $\mu=0.085,0.075,0.065,0.055$ (top to bottom, observed at the maxima). $a=20$, $q=0.0475$, and $\omega=0.2$ for all curves.

$$p\equiv(a+\mu t_n)^2/(2D_{c0}t_n) \ , \quad z_1\equiv(a+\mu t_n)/\sqrt{2\pi t_n} \ ,$$

$$b_1\equiv D_{c0}^{-2}+2a\mu D_{c0}^{-3} \ , \quad b_2\equiv 2D_{c0}^{-3}+6a\mu D_{c0}^{-4} \ .$$

For a fixed noise variance D, a particular peak tends to its maximum height for $\mu\to\mu_c$, where μ_c is defined by setting $nT_0=t_0$. (Note that this does *not* imply that this peak is the highest one in the histogram.) Thereafter, decreasing the noise variance further increases the height of the nth peak and, in the $D\to 0$ limit, the peak approaches a δ function. Hence the nth peak will have attained its maximum possible height in the singular limit $t_m\to t_0\approx nT_0$, corresponding to the confluence of three characteristic times in the system. In this limit, the multipeaked density function is supplanted by a single very narrow peak at nT_0. In practice these effects are somewhat difficult to observe because of the numerical problems encountered in plotting the FPTDF for extremely low noise variances. In Fig. 4 we plot the height of the fourth peak as a function of noise variance for different drift coefficients. As μ increases towards its critical value μ_c characterized by $t_0=4T_0$, the peak height increases and the critical noise strength (corresponding to the maximum in the peak height) approaches lower values. Figure 5 shows the effect of decreasing the noise, having set

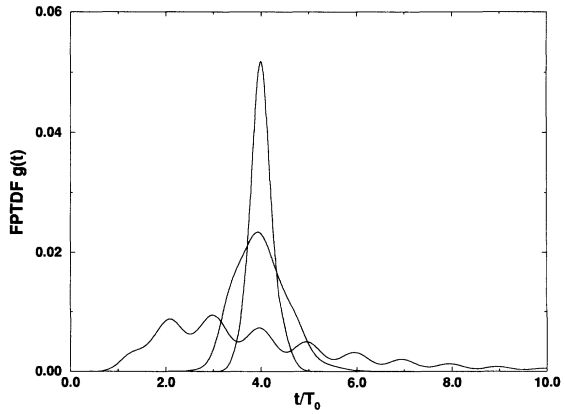

FIG. 5. FPTDF (7) showing increase in height of $n=4$ peak with decreasing noise variance. $\mu=0.159$ (critical value, see text) and $D=1.0$ (bottom curve), 0.06 (middle curve), and 0.012 (top curve). $a=20$, $q=0.0475$, and $\omega=0.2$ for all curves.

$\mu=\mu_c$. As the noise decreases, one approaches the $t_m=t_0$ limit. Since we already have set $t_0=4T_0$, the effect of decreasing the noise is to make the fourth peak the highest one in the FPTDF and, thereafter, to increase its height until it becomes a δ function in the singular limit, $D\rightarrow 0$, in which the three time scales coincide. The richness of behavior resulting from the coupling between the drift- and noise-dominated motions is evident in this subsection; we now demonstrate a somewhat different cooperative effect that is peculiar to this system.

B. Antiresonant behavior

One final property of the density function (7) is worth describing: the height at the mode of the density function (3) goes through a minimum as a function of noise. This can be shown by direct differentiation and has appeared in the literature [27]. The effect also occurs for the $q>0$ case. In Fig. 6 we plot this height as a function of noise variance D. The critical noise variance corresponding to the minimum turns out to be

$$D_m=\frac{a\mu}{2}+0.3512aq\ , \tag{15}$$

corresponding (for the $q=0$ case) to a mode that is exactly half the mean ($t_m=\frac{1}{2}t_0$). The second term in (15) has been obtained numerically. The behavior can be interpreted as a separation of regimes in which the random walk is dominated by drift and diffusion effects. In fact, one readily observes that $g_0(t_m)\approx(\mu^3/2\pi aD)^{1/2}$ for $D\ll a\mu/2$ whereas $g_0(t_m)\approx(3D/2a^2)(6/\pi e^3)^{1/2}$ in the opposite limit, corresponding to noise-dominated motion; in the transition region ($D\approx a\mu/2$), no clear behavior pattern emerges. In the $q>0$ case, one can set the parameters such that a particular peak is the highest. For a given drift and noise variance this amounts to setting the amplitude of the nth peak via expression (11) with nT_0 replaced by t_m, the mode, according to (10). This amplitude displays a minimum at a critical noise given by (15). Since the mode t_m depends on the noise, as we change D, we must change the frequency ω along with D if we desire the nth peak to be always the tallest one. Hence, for the modulated case, the above represents an adaptive change of parameters (the noise and frequency) such that the height of a given peak, always adjusted to be the tallest one in the FPTDF, passes through a minimum. This is shown in Fig. 7 in which the noise variance takes on three values, selected such that $g_0(t_m)$ passes through a minimum as a function of the noise. For each of these values the modulation frequency is adjusted, via the relation (10), so that the $n=3$ peak is the highest. The height of the third peak in the FPTDF then passes through a minimum as a function of these noise values, although it remains the highest peak in the FPTDF. The FPTDF $g_0(t)$ follows the same behavior as the $n=3$ peak of $g(t)$ for these parameter choices; this is as expected since, in plotting the curves of Fig. 7, we have selected two noise variances about the minimum defined by (15), held the drift constant, and adjusted the modulation frequency such that the relation (10) is satisfied in each case with $n=3$.

We can compare the properties of the FPTDF (7) with existing results from modulated noisy bistable systems. The multipeaked structure of the FPTDF, in the presence of the deterministic modulation, is well known in noisy bistable dynamic systems. It was first observed by Gammaitoni *et al.* in analog simulations [3] and has subsequently been described by numerous researchers in the nonlinear dynamics community [9,29]. Longtin, Bulsara, and Moss (LBM) [15] pointed out that depending on the measurement process, two density functions were possible in driven bistable systems; these consisted of peaks at the locations nT_0 (n integer) and $nT_0/2$ (n odd integer). They considered a "soft"-potential model of neuron dynamics and speculated that the second density function corresponded to the "hidden" or "reset" events that follow every neural firing; such events cannot be directly observed in neurophysiological experiments. However, the random walk model under consideration in this work differs from all the above treatments of bistable models in a very important respect. In the bistable model treatments of SR, the potential barrier cannot be crossed in the absence of noise, since the amplitude of the periodic modulation is taken to be too small to allow deterministic

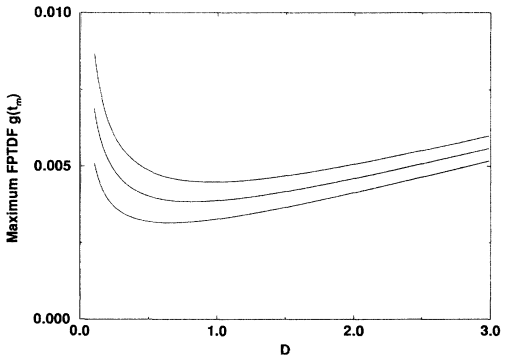

FIG. 6. Height of the FPTDF (7) at the mode vs noise variance for periodic stimulus amplitude $q=0$ (bottom curve), 0.01 (middle curve), and 0.05 (top curve). $a=20$ and $\mu=0.065$ for all curves.

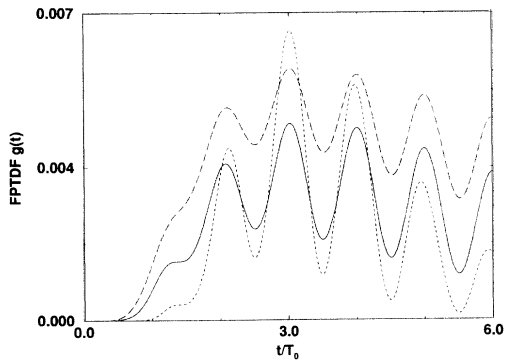

FIG. 7. "Antiresonant" behavior (see text) in the $n=3$ peak of the FPTDF. $D=0.195$ (dotted curve), 0.959 [solid curve; critical D as determined by (15)], and 2.702 (dashed curve). $a=20$, $\mu=0.065$, and $q=0.05$ for all curves, and modulation frequency ω is set, via the condition $t_m=3T_0$, such that the $n=3$ peak is the highest in each case.

switching. In the presence of a positive drift μ, however, the random walker considered in this work *will* reach the barrier in the absence of noise. This is reflected in a MFPT that does not depend on noise, in contrast with the Kramers rate that characterizes hopping events in bistable systems. However, this property also leads to the "antiresonant" behavior in the FPTDF that has been described in the preceding subsection; such behavior, which reflects a competition between the noise- and drift-dominated motion to the barrier, is not observed in bistable systems in which deterministic crossing events are forbidden. In bistable systems, the heights of peaks in the FPTDF display the same behavior that we observe in Fig. 3 [9,29]. Although there does not currently exist a precise frequency-matching condition that characterizes the "resonances" in the FPTDF peak heights, this effect has been espoused as a manifestation of SR at the level of the FPTDF in bistable systems, particularly since the hopping rate in such systems is noise dependent. No such significance can be attached to the behavior of Fig. 3 until we examine the spectral properties of the dynamics under consideration in this work; this is done in the following section.

III. SPECTRAL PROPERTIES OF THE DYNAMICS

The theory of the preceding section, as well as the other theories of noise-induced switching referred to above, demonstrate that the multipeaked structure of the FPTDF is a direct consequence of the noise. The LBM theory, in fact, invites speculation regarding the possible beneficial role of noise in sensory information processing. However, SR, characterized by a maximum in the output signal-to-noise ratio (SNR) vs noise-variance curve, has been demonstrated in a variety of physical experiments [6]. However, it has yet to be shown to play a fundamental role in sensory information processing in the nervous system, although there have been some experiments that show the characteristic SR behavior in neurons stimulated by periodic modulations superimposed on *externally* applied noise [30]. It is important to reiterate that the multipeaked FPTDF's that are ubiquitous in the neurophysiological literature are not (by themselves) indicators of SR as an underlying cooperative stochastic effect. To obtain such density functions it is sufficient to have some form of optimization process whereby certain system parameters, e.g., the potential barrier height in a bistable system or the quantities a and μ in the noisy dynamics, can be adjusted in response to the applied stimulus. Such an adjustment optimizes the coherence between the stimulus, which is assumed to carry external information, and the system response (characterized by the output signal strength S or the SNR). Although the peak heights in the FPTDF do display maxima as functions of the noise strength, attempts to quantify this "resonance" via a matching of two characteristic rates (as is the underlying precept in SR) have been largely inconclusive because of the practical difficulties associated with generating FPTDF's at low noise strengths.

The mathematical neurosciences literature contains several attempts to model neuron firing activity with an emphasis on stochastic point processes [25]. Generally, the focus has been on the FPTDF or ISIH. If the interspike intervals are assumed to be independent and identically distributed, then the point process is a *renewal* process [21,25]. It is important to point out that the FPTDF (or the ISIH) that was described in the preceding section is only one statistical measure of a point process; two different point processes may share identical FPTDF's. In addition, not all neurophysiological experiments yield FPTDF's that can be matched to the inverse Gaussian. Most conventional considerations of the response of these systems are based on an analysis of the power spectral density (PSD) characterizing the output; hence it seems reasonable to suppose that the two probabilistic measures of the response (the PSD and the FPTDF) should be related and in fact, for the case of a renewal process, they are known to be directly related. Accordingly, to understand better the cooperative behavior observed in the preceding section, we now consider the PSD of our model. We treat our modulated random walk as a renewal process, since the crossing times are independent of one another. This is possible because of our assumption of the phase resetting that accompanies the reset to the starting position, following each crossing of the barrier. Then, in terms of the FPTDF (8) we may write down the PSD at a frequency Ω [31]:

$$S(\Omega)=(\bar{T})^{-2}\delta(\Omega/2\pi)+(\bar{T})^{-1}\mathrm{Re}\left\{\frac{1+\phi(\Omega)}{1-\phi(\Omega)}\right\}, \quad (16)$$

where

$$\phi(\Omega)\equiv\int_0^\infty g(t)e^{i\Omega t}dt \quad (17)$$

is the characteristic function of the density function (7). At high frequencies, the PSD is seen to approach the limit $(\bar{T})^{-1}$ and at low frequencies, it approaches the limit $\{\mathrm{var}(T)\}/(\bar{T})^3$. In the absence of modulation we have the characteristic function

$$\phi_0(\Omega)=\exp\left\{\frac{a}{D}(\mu-\sqrt{\mu^2-2i\Omega D})\right\}, \quad (18)$$

which yields, combined with (15), the PSD at the frequency Ω corresponding to the $q=0$ case (the MFPT $\bar{T}$ is now replaced by t_0),

$$S_0(\Omega)=\frac{1-e^{2A}}{1+e^{2A}-2e^{A}\cos B}t_0^{-1}, \quad (19)$$

where we define

$$A\equiv\frac{a\mu}{D}-a\left[\frac{\sqrt{\mu^4+4\Omega^2D^2}+\mu^2}{2D^2}\right]^{1/2}, \quad (20a)$$

$$B\equiv\frac{a}{\sqrt{2}D}(\sqrt{\mu^4+4\Omega^2D^2}-\mu^2)^{1/2}. \quad (20b)$$

The behavior of the expression (19) as a function of the noise variance D is effectively dominated by the behavior of the real part of the characteristic function ϕ_0. We can write the real part of ϕ_0 in the form

$$\phi_{0r}\equiv e^{A}\cos B, \quad (21)$$

which we now analyze in some detail. To begin with we

note that $A \to 0$ in the $D \to 0$ and $D \to \infty$ limits; in between, it has a minimum at $D_e = (2+\sqrt{5})^{1/2}\mu^2/\Omega$. We observe that $B(D=0) = a\Omega/\mu$; thereafter it decreases to zero for increasing D. Hence the behavior of the relative maxima of ϕ_{0r} is determined by the parameter $\sigma = a\Omega/2\pi\mu \equiv t_0/T_0$, with $T_0 \equiv 2\pi/\Omega$ being the period corresponding to the frequency argument Ω in the PSD. A first-order expansion of ϕ_{0r} in D leads to the conclusion that for $\sigma < (\sqrt{2\pi})^{-1}$, ϕ_{0r} is decreasing at the origin, so that the only relative maximum for this case occurs for $D=0$. For $(\sqrt{2\pi})^{-1} < \sigma < \frac{1}{2}$, there is no relative maximum. For $\frac{1}{2} < \sigma < 1$ there is a relative maximum at $D=0$ since both terms in ϕ_{0r} are decreasing. For $\sigma \geq 1$, there is a relative maximum whenever $B = 2n\pi$ (n integer). In this case the number of relative maxima, N_m, is given by $N_m = [\sigma]$, i.e., the greatest integer not greater than σ. For the case $N_m \geq 1$, the relative maxima of ϕ_{0r} are very closely located by setting $B = 2n\pi$, which yields the critical noise variance $D_{\max}$ at which the maxima occur,

$$D_{\max} = \frac{a^2}{4n^2\pi^2}\sqrt{\Omega^2 - n^2\Omega_0^2}\,, \tag{22}$$

where $\Omega_0 \equiv 2\pi/t_0$. The actual maxima will be slightly displaced from these values because of the presence of the exponential in (19), but the displacement will be small since $0 \leq e^A \leq 1$. Note that, in (22), $n=1$ yields the "global" maximum, i.e., the one farthest from the origin. The actual maxima and minima can be easily found via expansion around $D_{\max}$ and D_e. Near the global maximum, characterized by $n=1$, the PSD (19) approaches the simple form,

$$S_0^{(m)} \equiv t_0^{-1}\frac{1+\exp(A_m)}{1-\exp(A_m)}\,, \tag{23}$$

with A_m obtained by substituting (20a) into (18):

$$A_m = 2\pi\frac{\Omega_0 - \Omega}{\Omega_0 + \Omega}\,. \tag{24}$$

The height of this maximum decreases with increasing a or decreasing μ. At the maximum, the PSD is characterized by only the two frequencies Ω and Ω_0. In what follows, and in the figures, we shall replace the PSD frequency Ω by ω whenever we specifically refer to an applied periodic stimulus of frequency ω.

In Fig. 8 we show (top curves) the signal strength $S(\omega)$ vs D, taken from the PSD for three modulation frequencies Ω. These curves are obtained numerically from the full FPT density (8). The bottom curves show the same cases but with $q=0$; these curves are calculated directly from the theory of the preceding paragraph. We note that the curves for $q>0$ are virtually identical (except for a vertical shift) to the $q=0$ case. For small q this is not surprising since, for the parameters considered in this work, the FPTDF is very well approximated by its first-order expansion in q. Hence much of the analysis that follows can be carried out for the simpler $q=0$ case and extended, qualitatively at least, to the $0 < q \ll \mu$ case. It is worth noting here that, in practice, we obtain very good results via the approximation (8) even for q approaching μ. The qualitative similarity in behavior of the spectral properties for the $q=0$ and $q>0$ cases is explicitly demonstrated in the figures. Decreasing the modulation frequency effectively makes the global maximum sharper and moves it to the left; these are characteristics of stochastic resonance as we know it in bistable systems. Note that if we take $\Omega = n\Omega_0$ there is a global maximum only at $D=0$ as shown by the analysis of the preceding paragraph.

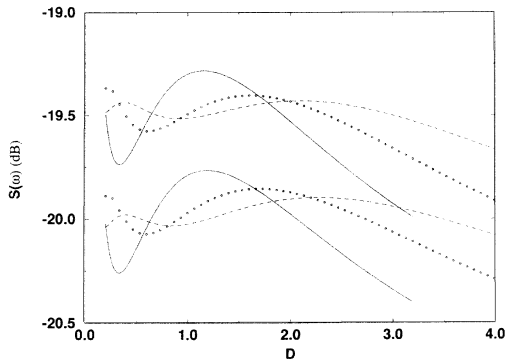

FIG. 8. Signal strength $S(\omega)$ of the PSD for three modulation frequencies ω, plotted as function of the nose variance D, with $q=0.025$ (top three curves), and 0 (bottom curves). $\omega = 0.125\,66$ (solid curves), 0.16 (open circles), and 0.2 (dashed curves). $a=20$ and $\mu=0.2$ for all curves.

Can the critical noise value (at the maximum) be expressed in terms of characteristic frequencies of the system as in conventional SR? We consider R, defined as the ratio of the mode location, given by (4), of the noise-only FPTDF to the modulation period T_0; with the mode being evaluated at the critical noise strength $D_{\max}$ given by (20) that approximately locates the global maxima of the curves in Fig. 8. After some algebra R becomes

$$R \equiv \left[\frac{t_m}{T_0}\right]_{D_{\max}} = \frac{3}{4\pi\Delta}\left\{\left[1+\Delta\left[\frac{16}{9}\pi^2 - 1\right]\right]^{1/2} - (1-\Delta)^{1/2}\right\}, \tag{25}$$

where we have introduced a parameter $\Delta \equiv \Omega_0^2/\Omega^2 \equiv T_0^2/t_0^2$ that is related to the detuning. As expected, $R \to 1$ as $\Delta \to 1$. The parameter Δ thus defines the critical point at which the global maximum of the signal strength vs noise curve occurs. Recall that the actual global maximum occurs at a location somewhat displaced from that predicted by (22). It is tempting to assume that this ability to express R solely as a function of the ratio Δ at the global maximum is a manifestation of SR. However, this is not necessarily the case, because we can calculate the "SNR" at the drive frequency Ω as a function of D directly from the curves in Fig. 8; for this purpose, we define the SNR to be the ratio of the PSD's at the frequency Ω in the presence and absence of the periodic modulation at that frequency. The result is a monotonically decreasing function; it does not go through a maximum. Hence, while the above-described effects may be an example of a nonlinear resonance that is controlled by

noise, they need not be taken to be the same as SR as we know it in bistable systems. Finally, the gain in signal strength as a function of noise is, at least for all the parameters chosen here, quite small (less than 1 dB). One can also plot the signal strength $S(\Omega)$ vs noise variance for different drift values, although this is not shown. Increasing the drift is seen to lead to a more pronounced maximum. This should be expected since the signal strength at a given frequency in the PSD will increase with the number of barrier crossing events.

The effects of changing the drift μ while keeping the noise constant are shown in Fig. 9, wherein we plot the signal strength at the drive frequency vs the drift for four different drive frequencies. The curves all go through maxima at critical values of the drift. Once again, the $q=0$ case yields curves that are virtually identical to the $q>0$ case except at very low μ, in which case the curves differ by a scale factor on the vertical axis. This is because with increasing μ the contribution of the second term in (8) to the FPTDF becomes increasingly negligible with the random walk becoming drift dominated. Hence, it is far more convenient to carry out our analysis based on the $q=0$ case. Note that, as Ω increases, the signal strength at the maximum increases; this is contrary to the results depicted in Fig. 8, in which the noise strength is varied instead of the drift. We also find that the critical drift (at the maximum) of any of these curves corresponds to a *matching of the drive period T_0 with the deterministic switching rate t_0*. This condition closely resembles the frequency-matching conditions that define conventional SR. In Fig. 10 we plot the ratios t_m/T_0 and t_m/t_0 vs the drift, keeping the noise variance D constant. The intersections of the curves yield the critical μ values at which the peaks in Fig. 8 occur. A far more interesting situation is shown in Fig. 11. Here we plot the signal strength at a given frequency $\Omega=\omega$ vs drift, and change the noise variance. Once again we obtain global maxima for μ values corresponding to $T_0=t_0$. However, we also notice the appearance of an additional peak in the signal strength for low applied noise which occurs at $T_0=t_0/2$. This effect can be explained by returning to Eq. (22) and inverting to obtain the dependence of μ on D. We readily

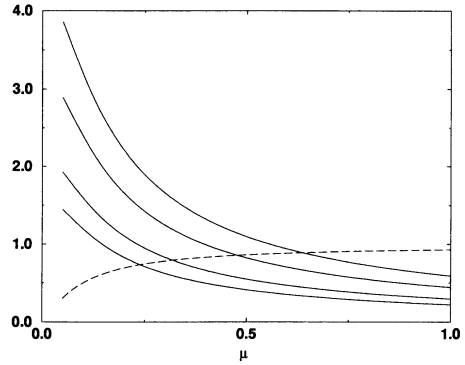

FIG. 10. Ratios t_m/T_0 (solid curves) for $\omega=0.075$, 0.1, 0.15, and 0.2 reading from bottom to top and t_m/t_0 (dashed curve), vs drift μ. The intersections yield locations of the maxima in Fig. 9. $a=20$, $q=0.025$, and $D=1$ for all curves.

find that

$$\Omega_0=\frac{1}{n}\left[\Omega^2-\frac{16n^4\pi^4D^2}{a^4}\right]^{1/2}, \tag{26}$$

where we recall that $\Omega_0=2\pi\mu/a$. This expression will have a real root for $D<a^2\Omega/4n^2\pi^2$. For the case when $\Omega>4\pi^2D/a^2$, one can always find an $n\geq 1$ such that the argument of the square root in (26) is positive. Then $n=1$ defines the global or *dominant* maximum of the signal strength, corresponding to the largest μ value. For large a, the second term in the square root can be neglected (for small n) and we have the dominant maximum occurring at $\Omega_0=\Omega$, i.e., $T_0=t_0$; this is also the maximum that corresponds to the largest μ value. The next lower maximum occurs for $n=2$ ($T_0=t_0/2$) and so on. In fact, one obtains a local maximum for all integer n values until the argument of the square root turns negative. Interestingly, the function $\cos B$ in (19), and therefore also the real part ϕ_{0r} of the characteristic function, both have maxima at the same n values. For large a, the first few maxima correspond very well to the condition $nT_0=t_0$ [given by the first term in the square root of (26)]

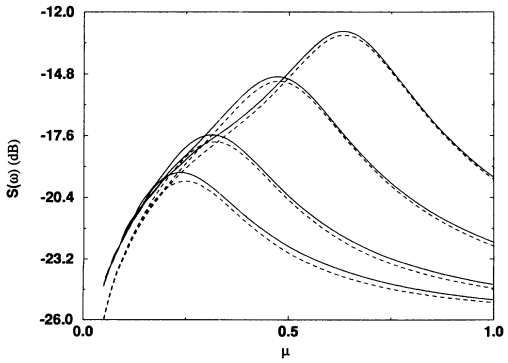

FIG. 9. Signal strength $S(\omega)$ vs drift μ for (reading the sets of curves from bottom to top) $\omega=0.075$,0.1,0.15,0.2. Solid and dashed curves in each set correspond to $q=0.025$ and $q=0$, respectively. $a=20$ and $D=1$ for all curves.

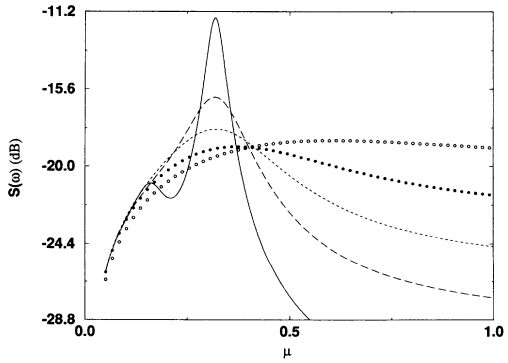

FIG. 11. Signal strength $S(\omega)$ vs μ for noise variance $D=0.15$ (solid curve), 0.5 (large dashes), 1.0 (dots), 2.0 (filled circles), and 4.0 (open circles). $a=20$, $q=0.025$, and $\omega=0.1$ for all curves.

which was precisely the condition for the nth peak in the FPTDF to attain its maximum height for a fixed noise variance D. However, as n increases, the second term in the square root of (26) becomes non-negligible and the maxima are determined via the full condition (26). In Fig. 12 we show a case with multiple maxima. Here $a=60$ and one expects to find $n=9$ maxima. However, the amplitudes of the maxima decrease rapidly with increasing n and the low-lying ones cannot be resolved on the scale of the figure. These curves are computed directly from Eq. (19) for the signal strength in the absence of the modulation; however, a full numerical simulation of the dynamics of (1) with a small modulation amplitude q (compared to the drift μ) yields qualitatively similar behavior. The small differences between the $q=0$ and $q>0$ cases are evidenced solely in a vertical scale factor as stated earlier. The values of the drift μ corresponding to the maxima of Fig. 12 are well approximated by the condition (26) with the second term in the square root neglected for small n. From the foregoing discussion, it is evident that the dominant maximum (the farthest one) occurs at $T_0/t_0 \equiv T_0\mu/a=1$; thereafter the maxima occur approximately at $T_0/t_0=\frac{1}{2},\frac{1}{3},\frac{1}{4},\ldots$. The effect of changing the noise variance is also shown in this figure; lowering D leads to the appearance of more peaks together with an increase in the peak amplitude. In fact, a given peak, in Fig. 12, attains its maximum possible height in the $D\to 0$ limit corresponding to the $t_m \to t_0$ case; this is precisely the limit, discussed in the preceding section, in which the nth peak in the FPTDF approaches a δ function. For both noise values, the dominant maxima occur for the same μ value; they correspond to $n=1$ and $T_0 \approx t_0$, a condition that is basically independent of the noise variance. As n increases, the second term in (26) becomes increasingly important in computing the critical values of μ, and the peak locations are no longer determined via the condition $\Omega_0=\Omega/n$. We can compute exactly the signal strength $S_0^{(n)}$ for any discrete value of n, yielding the signal strength at the peaks in Fig. 12, by substituting (22) into (17). After some calculation we obtain

$$S_0^{(n)} \equiv t_0^{-1} \frac{1+\exp(A_n)}{1-\exp(A_n)} , \tag{27}$$

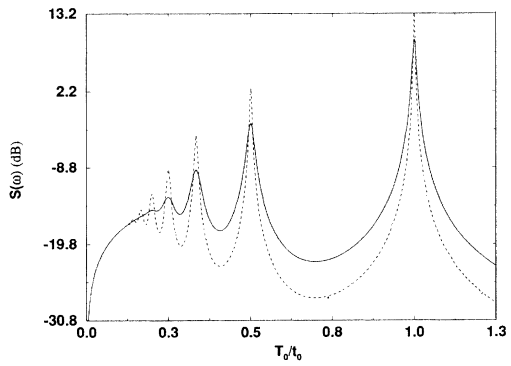

FIG. 12. Signal strength $S(\omega)$ vs T_0/t_0 calculated directly from (19) with $q=0$. $D=1.0$ (solid curve) and 0.3 (dashed curve). $a=60$ and $\Omega=1.0$ for both curves.

where

$$A_n = \frac{a^2\Omega}{2n\pi D}\left[\left|1-\frac{16n^4\pi^4D^2}{a^4\Omega^2}\right|^{1/2}-1\right] . \tag{28}$$

The $n=1$ peak is the highest one. Also, $S_0^{(n)}$ increases with increasing frequency Ω, as was observed in Fig. 9. For large D values such that the square root in (26) is imaginary for $n=1$, we *still* observe a (single) maximum in the signal strength. Two such cases are shown in Fig. 11 ($D=2,4$). For these higher D values, the factor $\cos B$ in (19) has only a single, global, minimum and both the factors in (21) determine the location of the extrema of $S(\Omega)$, in contrast to the cases discussed above wherein the extrema of $\cos B$ yield the extrema of $S(\Omega)$ to a high degree of accuracy. As D increases with a and Ω held constant the peak becomes noticeably less sharp and the signal strength approaches a plateau.

To summarize, the preceding paragraph has established a connection between the limiting behavior of the peaks in the signal strength and the FPTDF (8). If we consider the FPTDF as a function of the drift μ, then for $\mu=\mu_c \equiv a\Omega/2n\pi$ it consists of a single, very sharp peak located at $t/T_0=n$. For small deviations from μ_c, this peak is shifted from this location and its height decreases. In fact, we have already seen that, for a given a, q, Ω, and D, the nth peak in the FPTDF attains its maximum height at a drift determined by $t_0(=a/\mu)=nT_0$, in connection with Fig. 4. This condition sets the location of the mean of the FPTDF, which is precisely the condition for determining the locations of the peaks in Figs. 11 and 12. Having fixed the value of μ, the effect of changing the noise variance D is to render the FPTDF peak sharper and taller for decreasing D, which ultimately leads to the singular limit $t_0=nT_0 \approx t_m$ discussed in the preceding section, or broader and lower for increasing D. Precisely this behavior is observed in the signal strength as shown in Fig. 12 for two D values. We have thus established a connection between the FPTDF (8) and the behavior of the signal strength $S(\Omega)$ which is obtained directly from the PSD. Changing the frequency yields curves that are qualitatively similar to Figs. 11 and 12 except that the locations and numbers of the peaks change. The maximum number of peaks allowed for a given Ω is contingent on the argument of the square root being non-negative. On a graph with T_0/t_0 as the abscissa, the resolvable or visible peaks occur at identical locations. Although the number of peaks may differ for different Ω values, the lower-lying peaks are not resolvable on the scale of the figure; their amplitudes may, however, be different for different Ω values.

IV. CONCLUDING REMARKS

The behavior described in this work certainly has the flavor of stochastic resonance; however, we are reluctant to assign these effects to the same class as the cooperative behavior that is seen in driven bistable systems, although it may have much in common with existing observations on SR in simple systems as described in Sec. I. Certainly major differences exist between the characterization of our problem and of bistable systems in the study of

noise-induced cooperative behavior. One such difference is the introduction of a positive drift in our problem; this effectively removes the restrictive lack of deterministic switching that is commonly used to constrain bistable systems. We do, however, impose a constraint, the assumption that the periodic-stimulus-induced motion is a small perturbation to the drift-driven dynamics, which may be regarded as the counterpart of the proscription against deterministic switching in bistable model treatments. Despite this assumption, a passage to the boundary is guaranteed in our problem, even in the absence of noise, because of the positive drift. In fact, we observe that the drift significantly affects the response of the system, and the competition between the drift- and noise-dominated motion introduces some very interesting behavior. The simplicity of this model (most of the calculations can be done analytically) permits us to establish a connection between the rich cooperative behavior observed at the level of the FPTDF and the PSD; a precise connection of this kind has not been possible in bistable systems because of the difficulty in performing simulations at low noise strengths. That the critical quantity R [Eq. (25)] can be expressed solely in terms of the frequencies Ω and Ω_0 points to the cooperative effects as being strongly frequency dependent, and it is important to note that no approximation similar to the adiabatic approximation [3], that is frequently made in bistable dynamics, has been made here. Nonetheless, the fact that we obtain qualitatively similar behavior to SR as it is commonly observed in bistable systems when we consider the output signal strength, but do not see the SNR (defined in Sec. II) passing through a maximum, gives us reason to treat this effect as a somewhat different type of "resonance."

With regard to the neurophysiological ramifications of this work, it is important to observe that the FPTDF's of Sec. II, for the $q>0$ case, cannot exist in the absence of noise. The results of that section seem to point to the existence of a selection mechanism whereby the response to a deterministic periodic stimulus, whose frequency is its most important aspect, is enhanced by background noise, using the distance to the firing threshold (the absorbing boundary in our current system) as a "control parameter" that can be internally adjusted. To obtain well-defined multipeaked histograms such as we show in Fig. 2, one must have the system and stimulus parameters constrained within certain well-defined ranges. Then, increasing the drift or decreasing the noise variance leads to a dominant response at a particular harmonic; the response is a maximum at the confluence of the three times t_m, t_0, and nT_0, as described in Sec. II. This model and other, bistable, models embodying SR are open to the criticism that information may be lost in our considerations of these models as purely threshold devices, with all details regarding the passage to the threshold being neglected. Nevertheless these models reproduce (qualitatively, at least) remarkably similar behavior, in the FPTDF, to what is observed in experiments; in fact, the model (1) with $\lambda=0$ has been shown to reproduce some of the salient features observed in recordings from periodically stimulated cortical neurons [32].

ACKNOWLEDGMENTS

We warmly acknowledge discussions with Dr. C. Hicks, Dr. R. Boss, and Dr. E. Jacobs (NCCOSC) as well as Dr. L. Gammaitoni (Perugia), Dr. P. Jung (Augsburg and Illinois), Dr. R. Fox and Dr. K. Wiesenfeld (Georgia Tech.), Dr. L. Kiss (Uppsala), Dr. F. Moss (St. Louis), Dr. K. Pribram (Radford), Dr. H. Tuckwell (Canberra), Dr. P. Lansky (Prague), and Dr. K. Pakdaman (Paris). The work would not have been possible without support from the Physics Division of the Office of Naval Research; this support is gratefully acknowledged.

[1] R. Benzi, A. Sutera, and A. Vulpiani, J. Phys. A **14**, L453 (1981); J-P. Eckmann, L. Thomas, and P. Wittwer, *ibid.* **14**, 3153 (1981); J-P. Eckmann and L. Thomas, *ibid.* **15**, L261 (1982).

[2] C. Nicolis and G. Nicolis, Tellus **33**, 225 (1981); C. Nicolis, *ibid.* **34**, 1 (1982); R. Benzi, G. Parisi, A. Sutera, and A. Vulpiani, *ibid.* **34**, 10 (1982); SIAM J. Appl. Math. **43**, 565 (1983).

[3] B. McNamara and K. Wiesenfeld, Phys. Rev. A **39**, 4854 (1989); L. Gammaitoni, F. Machesoni, E. Menichaella-Saetta, and S. Santucci, Phys. Rev. Lett. **62**, 349 (1989); Phys. Rev. A **40**, 2114 (1989).

[4] P. Jung and P. Hanggi, Europhys. Lett. **8**, 505 (1989); Phys. Rev. A **44**, 8032 (1991).

[5] M. Dykman, P. McClintock, R. Manella, and N. Stocks, Pis'ma Zh. Eksp. Teor. Fiz. **52**, 780 (1990) [JETP Lett. **52**, 141 (1990)].

[6] S. Fauve and F. Heslot, Phys. Lett. **97A**, 5 (1983); B. McNamara, K. Wiesenfeld, and R. Roy, Phys. Rev. Lett. **60**, 2626 (1988); G. Vemuri and R. Roy, Phys. Rev. A **39**, 4668 (1989); L. Gammaitoni, F. Marchesoni, M. Martinelli, L. Pardi, and S. Santucci, Phys. Lett. A **158**, 449 (1991); V. Anischenko, M. Safanova, and L. Chua; Int. J. Bifurc. Chaos **2**, 392 (1992); M. Spano, M. Wun-Fogle, and W. Ditto, Phys. Rev. A **46**, 5253 (1992); A. Hibbs, E. Jacobs, J. Bekkedahl, A. Bulsara, and F. Moss, in *Noise in Physical Systems and* $1/f$ *Fluctuations,* edited by P. Handel and A. Chung (AIP, New York, 1993); J. Grohs, S. Apanasevich, P. Jung, H. Isler, D. Burak, and C. Klingshirn, Phys. Rev. E **49**, 2199 (1994).

[7] T. Zhou and F. Moss, Phys. Rev. A **39**, 4323 (1989); G. De-chun and H. Gang, *ibid.* **46**, 3243 (1992).

[8] F. Moss, in *An Introduction to Some Contemporary Problems in Statistical Physical Physics,* edited by G. Weiss (SIAM, Philadelphia, 1994).

[9] P. Jung, Phys. Rep. **234**, 175 (1994).

[10] F. Moss, A. Bulsara, and M. Schlesinger, *Proceedings of the NATO Advanced Research Workshop on Stochastic Resonance in Physics and Biology* [J. Stat. Phys. **70** (1/2) (1993)].

[11] A. Bulsara, E. Jacobs, T. Zhou, F. Moss, and L. Kiss, J. Theor. Biol. **152**, 531 (1991); C. Doering and J. Gadoua,

Phys. Rev. Lett. **69**, 2318 (1992); R. Bartussek, P. Jung, and P. Hanggi, in *Noise in Physical Systems and 1/f Fluctuations,* edited by P. Handel (AIP, New York, 1993); U. Zurcher and C. Doering, Phys. Rev. E **47**, 3862 (1993); L. Gammaitoni, F. Marchesoni, E. Menichaella-Saetta, and S. Santucci, *ibid.* (this issue) **49**, 4878 (1994); P. Hanggi (unpublished); R. Bartussek, P. Hanggi, and P. Jung, Phys. Rev. E (to be published).

[12] H. Gang, H. Haken, and C. Ning, Phys. Lett. A **172**, 21 (1992); Phys. Rev. E **47**, 2321 (1993); T. Carroll and L. Pecora, Phys. Rev. Lett. **70**, 576 (1993); Phys. Rev. E **47**, 3941 (1993); H. Gang, T. Ditzinger, C. Ning, and H. Haken, Phys. Rev. Lett. **71**, 807 (1993); L. Gammaitoni, F. Marchesoni, E. Menichaella-Saetta, and S. Santucci, *ibid.* **71**, 3625 (1993).

[13] P. Jung, U. Behn, E. Pantazelou, and F. Moss, Phys. Rev. A **46**, 1709 (1991); L. Kiss, Z. Gingl, Z. Marton, J. Kertesz, F. Moss, G. Schmera, and A. Bulsara, J. Stat. Phys. **70**, 451 (1993); E. Pantazelou, F. Moss, and D. Chialvo, in *Noise in Physical Systems and 1/f Fluctuations* (Ref. [11]).

[14] A. Bulsara and G. Schmera, Phys. Rev. E **47**, 3734 (1993); A. Bulsara, A. Maren and G. Schmera, Biol. Cybern. **70**, 145 (1993); A. Bulsara and A. Maren, in *Rethinking Neural Networks: Quantum Fields and Biological Data,* edited by K. H. Pribram (Erlbaum, Hillsdale, NJ, 1993).

[15] A. Longtin, A. Bulsara, and F. Moss, Phys. Rev. Lett. **67**, 656 (1991) [see also Nature (London) **352**, 469 (1991)]. A Bulsara and F. Moss, in *Proceedings of the Meeting on Noise in Physical Systems and 1/f Fluctuations ICNF91,* edited by T. Musha, S. Sato, and Y. Yamamoto (Omsha, Tokyo, 1991); A. Longtin, A. Bulsara, and F. Moss, Mod. Phys. Lett. B **6**, 1299 (1992); A. Longtin; Center Nonlin. Studies Newsl. **74** (1992) [Los Alamos National Laboratory Report No. LA-UR-92-163, 1992 (unpublished)]; A. Longtin, J. Stat. Phys. **70**, 309 (1993); A. Longtin, A. Bulsara, D. Pierson, and F. Moss; Biol. Cybern. **70**, 569 (1994).

[16] K. Wiesenfeld, D. Pierson, E. Pantazelou, C. Dames, and F. Moss, Phys. Rev. Lett. **72**, 2125 (1994).

[17] M. Gitterman and G. Weiss, J. Stat. Phys. **70**, 107 (1993); N. Stocks, N. Stein, and P. McClintock, J. Phys. A **26**, L85 (1993).

[18] E. Fletcher, S. Havlin, and G. Weiss, J. Stat. Phys. **51**, 215 (1988).

[19] See, e.g., E. Montroll, in *Proceedings of Symposia in Applied Mathematics* (American Mathematical Society, Providence, RI, 1964), Vol. 26; E. Montroll and M. Shlesinger, in *Studies in Statistical Mechanics,* edited by E. Montroll and J. Lebowitz (North-Holland, Amsterdam, 1984), Vol. II, and references therein.

[20] A. Siegert, Phys. Rev. **81**, 617 (1951); D. Darling and A. Siegert, Ann. Math. Stat. **24**, 624 (1953).

[21] A. Bharucha-Reid, *Elements of the Theory of Markov Processes and their Applications* (McGraw-Hill, New York, 1960); D. Cox and H. Miller, *The Theory of Stochastic Processes* (Chapman and Hall, London, 1965); W. Feller, *An Introduction to Probability Theory and its Applications* (Wiley, New York, 1971), Vol. 2; I. Blake and W. Lindsey. IEEE Trans. Inf. Theory **IT-19**, 295 (1973).

[22] G. Uhlenbeck and L. Ornstein, Phys. Rev. **36**, 823 (1930); S. Chandrasekhar, Rev. Mod. Phys. **15**, 1 (1943); M. Wang and G. Uhlenbeck, Rev. Mod. Phys. **17**, 323 (1945); M. Kac, in *Selected Papers on Noise and Stochastic Processes,* edited by N. Wax (Dover, New York, 1954).

[23] B. Knight, J. Gen. Physiol. **59**, 734 (1972); R. Cappocelli and L. Ricciardi, J. Theor. Biol. **40**, 369 (1973); J. Clay and N. Goel, *ibid.* **39**, 633 (1973); J. Cowan, in *Statistical Mechanics,* edited by S. Rice, K. Freed, and J. Light (University of Chicago Press, Chicago, 1974); A. Holden, *Models of the Stochastic Activity of Neurons* (Springer-Verlag, Berlin, 1976); L. Ricciardi, *Diffusion Processes and Related Topics in Biology* (Springer-Verlag, Berlin, 1977); C. Ascoli, M. Barbi, S. Chilemmi, and D. Petracchi, Biophys. J. **19**, 219 (1977); P. Lansky, J. Theor. Biol. **107**, 631 (1984); P. Lansky and T. Radil, Biol. Cybern. **55**, 299 (1987); L. Ricciardi and S. Sato; J. Appl. Prob. **25**, 43 (1988); P. Johannesma, in *Neural Networks,* edited by E. Caianello (Springer-Verlag, Berlin, 1988); C. Smith, in *Single Neuron Computation,* edited by T. McKenna, J. Davis, and S. Zornetzer (Academic, New York, 1992).

[24] J. Keener, F. Hoppenstaedt, and J. Rinzel, SIAM J. Appl. Math. **41**, 503 (1981).

[25] H. Tuckwell, *Stochastic Processes in the Neurosciences* (SIAM, Philadephia, 1979); *Introduction to Theoretical Neurobiology* (Cambridge University Press, Cambridge, England, 1988), Vol. 2.

[26] G. Gerstein and B. Mandelbrot, Biophys. J. **4**, 41 (1964).

[27] R. Chikara and L. Folks, *The Inverse Gaussian Distribution* (Dekker, New York, 1989).

[28] C. Stevens, Biophys. J. **4**, 417 (1964).

[29] T. Zhou, F. Moss, and P. Jung, Phys. Rev. A **42**, 3161 (1990).

[30] J. Douglass, F. Moss, and A. Longtin, in *Advances in Neural Information Proceedings Systems,* edited by S. Hanson, J. Cowan, and L. Giles (Morgan Kauffman, San Mateo, CA, 1993), Vol. 4; D. Chialvo and A. Apkarian, J. Stat. Phys. **70**, 375 (1993); A. Bulsara, J. Douglas, and F. Moss, Nav. Res. Rev. **45**, 23 (1993); J. Douglass, L. Wilkens, E. Pantezelou, and F. Moss, Nature (London) **365**, 337 (1993).

[31] T. Lukes, Proc. Phys. Soc. London **78**, 153 (1961); S. Lowen, Ph.D. dissertation, Columbia University, 1992, Chap. 3; S. Lowen and M. Teich, Phys. Rev. E **47**, 992 (1993).

[32] R. Siegal and H. Read, J. Stat. Phys. **70**, 297 (1993).